ELSEVIER

Journal of Nuclear Materials 247 (1997) 98–102

journal of nuclear materials

Study on order–disorder transition of Hf–O alloys (O/Hf = 0.11 – 0.22) by heat capacity measurement

Tetsuya Kato *, Toshihide Tsuji

Department of Nuclear Engineering, Faculty of Engineering, Nagoya University, Furo-Cho, Chikusa-ku, Nagoya 464-01, Japan

Abstract

The heat capacities of hafnium–oxygen solid solutions, HfO_X ($X = 0.11$, 0.19 and 0.22), were measured from 325 to 905 K by using an adiabatic scanning calorimeter. Entropy changes due to the order–disorder transition of the oxygen sublattice were estimated from the heat capacity data in this study and were recomputed for HfO_X ($X = 0.14$ and 0.17) whose heat capacities had been measured in our previous study. The experimental transition entropy change obtained for the composition of $X = 0.17$ ($\approx 1/6$) was in good agreement with the theoretical transition entropy change calculated on the basis of the crystal analyses using statistical thermodynamics, while the experimental values for the other compositions ($X \neq 0.17$) were smaller than the theoretical values. The difference between the experimental and theoretical values was considered to be caused by the increasing degree of configurational freedom in the ordered structures due to the increments of oxygen vacancies for $X < 1/6$ or the increments of interstitial oxygen atoms for $X > 1/6$. © 1997 Elsevier Science B.V.

1. Introduction

It is known that the interstitial oxygen atoms dissolved in titanium and zirconium metals form ordered structures in low temperatures and cause order–disorder transitions between 600 and 800 K. We have measured the heat capacities of titanium–oxygen [1] and zirconium–oxygen [2] solid solutions and discussed the order–disorder behaviors of the oxygen atoms in view of statistical thermodynamics by referring to the experimental transition entropy changes computed from measured heat capacities.

Hafnium also belongs to the same IVA group as titanium and zirconium metals. Oxygen dissolves in hafnium metal up to 20 at.% (O/Hf = 0.25) [3,4] and these dissolved interstitial oxygen atoms form ordered structures similar to those of titanium- and zirconium–oxygen solid solutions [5]. Hirabayashi et al. [6] determined the ordered structures of hafnium–oxygen solid solutions, HfO_X, by using electron and neutron diffraction methods. They reported that the basic ordered structures of HfO_X was the ordered one for $X = 1/6$ and oxygen vacancies for $X < 1/6$ or interstitial oxygen atoms for $X > 1/6$ existed in the basic ordered structure. Moreover, they measured the heat capacities of HfO_X ($X = 0.11$ to 0.23), but the experimental transition entropy changes computed from their heat capacity data were smaller than the theoretical values calculated on the basis of their crystal structure analyses. We also measured heat capacities of HfO_X ($X = 0.14$, 0.17 and 0.19) alloys from 325 to 905 K by using an adiabatic scanning calorimeter [7]. In our previous work, the experimental transition entropy changes computed from the heat capacity data were larger than those reported by Hirabayashi et al. [6] and the experimental values for the composition of $X = 0.14$ and 0.17 were in good agreement with the theoretical values. However, for $X = 0.19$, the experimental value was smaller than the theoretical one and the shape of the heat capacity curve was different from those for HfO_X ($X = 0.14$ and 0.17), TiO_X [1] and ZrO_X [2].

In this paper, we describe the results of heat capacity measurements of HfO_X, $X = 0.11$ and 0.22, from 325 to 905 K by using an adiabatic scanning calorimeter together with that of $X = 0.19$ measured again after annealing and

* Corresponding author. Present address: Nuclear Fuel Cycle Department, Central Research Institute of Electric Power Industry, Iwadokita 2-Chome 11-1, Komae-shi, Tokyo 201, Japan. Tel.: +81-3 3480 2111; fax: +81-3 3480 7956; e-mail: tkato@criepi.denken.or.jp.

0022-3115/97/$17.00
PII S0022-3115(97)00095-0

discuss the transition mechanism in the wide composition range by comparing the experimental entropy changes of the order–disorder transition with the theoretical values from the view point of statistical thermodynamics, including the recomputed experimental values of the compositions of $X = 0.14$ and 0.17 measured in the previous study [7].

2. Experimental

The experimental procedure in this study has been described previously [7]. In this study, we prepared HfO_X with compositions of $X = 0.11$ and 0.22. For $X = 0.19$, the sample prepared in the previous study was used in the measurement after reannealing. It was confirmed from an X-ray diffraction method that both prepared alloys were single phase having a hexagonal crystal structure of α-Hf. The composition of each alloy was determined from weight gain in oxidization to hafnium dioxide, HfO_2. The determined compositions were in nearly good agreement with the initial compositions. To fabricate the samples for heat capacity measurements, the prepared alloys were crushed into pieces of less than 3 mm in size and about 36 g of each alloy was sealed in each quartz vessel with a helium gas pressure of 20 kPa (150 Torr).

The heat capacity measurements of HfO_X ($X = 0.11$, 0.19 and 0.22) were carried out using an adiabatic scanning calorimeter from 325 to 905 K as described elsewhere [1,2,7]. The scanning heating rate chosen in this study was 2 K min^{-1}. Heat capacity measurements using the calorimeter were standardized by carrying out measurements on pure zirconium metal. In comparison with the reliable data of Douglas [8], the imprecision and the inaccuracy were determined to be $+5\%$ and $\pm 3\%$, respectively.

We carried out the heat capacity measurements in the following procedure to obtain the experimental transition entropy changes. At first, measurements were carried out on the samples without any annealing. These heat capacity data were used for determinations of the base lines required to estimate the experimental transition entropy changes as described later. Then, the samples were annealed at the appropriate temperature between 603 and 623 K for 2 weeks to form the ordered structures in the interstitial oxygen sublattice and cooled slowly for 1 week to ambient temperature. Finally, heat capacities were measured on these annealed samples with the ordered structures and we obtained the experimental transition entropy changes.

3. Results and discussion

The results of the heat capacity measurements on HfO_X ($X = 0.11$, 0.19 and 0.22) before annealing (without any annealing) and after annealing are shown in Figs. 1 and 2, respectively, together with the results of our previous measurements ($X = 0.14$ and 0.17) [7]. In all measurements, the heat capacity anomalies due to the order–disorder transition are seen around 700 K. Of course, the peak area for samples before annealing is much smaller than that for the samples after annealing because the ordered structures in the samples before annealing had not been formed completely at the start of measurement, so the transition enthalpy and entropy changes have to be estimated using the heat capacity data in Fig. 2.

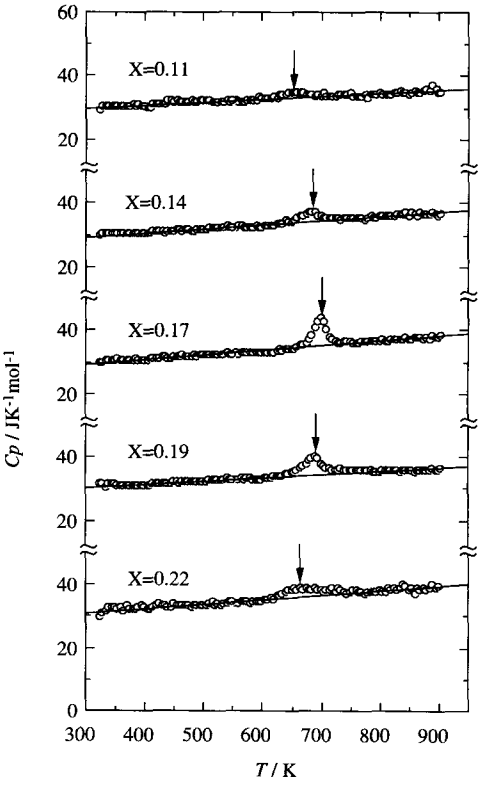

Fig. 1. Heat capacities of HfO_X in this study ($X = 0.11$, 0.19 and 0.22) and our previous work ($X = 0.14$ and 0.17) [7] before annealing. The solid lines are the base lines determined by fitting heat capacity data excluding the heat capacity anomaly due to the order–disorder transition to a straight line. The arrows indicate transition temperatures.

In Fig. 2, other heat capacity anomalies are seen in the lower temperature range up to 600 K for all samples, although this anomaly was not observed for the heat capacity measurement on $X = 0.19$ in our previous study [7]. Similar heat capacity anomalies have been observed for titanium–oxygen [1], zirconium–oxygen [2] and hafnium–oxygen [7] solid solutions and we referred to it as the low temperature heat capacity anomaly in the previous paper [1,2,7]. On the other hand, the low temperature heat capacity anomalies are not seen in Fig. 1 for the samples

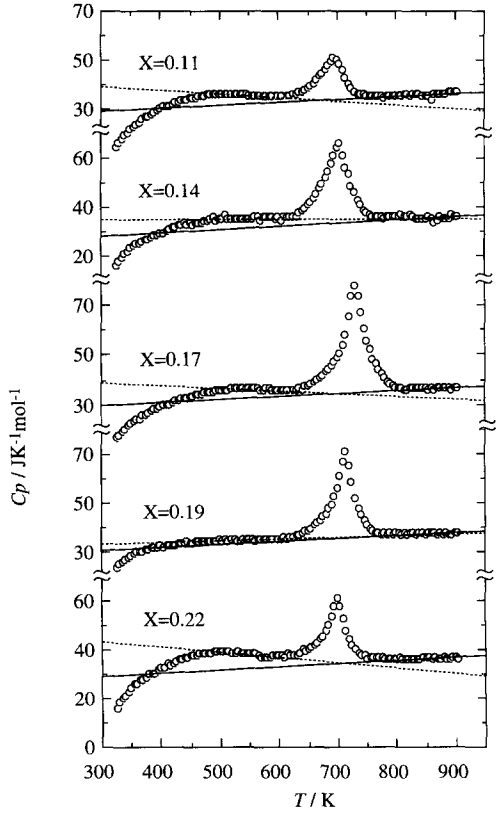

Fig. 2. Heat capacities of HfO_X in this study ($X = 0.11$, 0.19 and 0.22) and our previous work ($X = 0.14$ and 0.17) [7] after annealing. The solid lines are the base lines of the heat capacity curves. The dotted lines are the attenuation lines of the low temperature heat capacity anomaly.

before annealing. We assumed that the low temperature heat capacity anomaly was caused by poor heat conduction in a quartz vessel due to lowering the helium gas pressure during annealing. In order to check this possibility, we performed a series of simple experiments. At first, we measured the heat capacity on a sample resealed with a helium gas pressure of 20 kPa after we confirmed the existence of a low temperature heat capacity anomaly. As expected, the low temperature heat capacity anomaly disappeared and this heat capacity curve looked like heat capacity curves in Fig. 1. In the next step, we measured the heat capacity on a sample evacuated and sealed again in a quartz vessel after we confirmed no existence of the low temperature heat capacity anomaly. As a result, an anomaly similar to the low temperature heat capacity anomaly appeared again. Heat capacity measurement on pure zirconium metal evacuated and sealed in a quartz vessel was also carried out and an anomaly similar to the low temperature heat capacity anomaly was observed as expected. From these experimental facts, our assumption seems to be true. We could not examine the reason why the helium gas pressure lowered during annealing. Considering that IVA metals have the property of dissolving a large amount of light elements, e.g., hydrogen, carbon, nitrogen and oxygen, some of the helium may be absorbed in the hafnium–oxygen solid solution during annealing. It seems to be caused by a slightly lower annealing temperature that the low temperature heat capacity anomaly not observed for the measurement of $X = 0.19$ after annealing in our previous study.

In order to compute the experimental transition enthalpy and entropy changes from heat capacity data in this study, the appropriate peak area due to the order–disorder transition has to be determined excluding the effect of the low temperature heat capacity anomaly. So in this study, two lines are determined as shown in Fig. 2. One is the attenuation line of the low temperature heat capacity anomaly shown as the dotted lines and the other is the base line of heat capacity curve shown as the solid lines. The attenuation lines were determined by fitting heat capacity data to a straight line in the appropriate part of the low temperature heat capacity anomaly in Fig. 2, because it was found that the low temperature heat capacity anomaly attenuated along by a straight line from the heat capacity measurement of pure zirconium metal evacuated and sealed in a quartz vessel which was needed for the examination of low temperature heat capacity anomaly. The base lines of heat capacity curves were determined by solid lines shown in Fig. 1 as described previously [7]. The solid lines in Fig. 1 were determined by fitting heat capacity data to a straight line excluding the heat capacity anomaly due to the order–disorder transition. Then, for each heat capacity curve in Fig. 2, we determined the base line that had the average slope of the solid lines in Fig. 1 and the minimum standard deviation from heat capacity data in the high temperature range above 830 K uninfluenced by the order–disorder transition in Fig. 2. We can obtain the experimental transition enthalpy and entropy changes by integrating the area enclosed by heat capacity curve, the attenuation line and the base line in Fig. 2.

The order–disorder transition temperatures, enthalpy changes and entropy changes obtained in this study are shown in Fig. 3(a)–(c), respectively, as a function of the O/Hf atomic ratio, or X in HfO_X with those obtained previously by Hirabayashi et al. [6]. The temperatures corresponding to the maximum heat capacity peak for samples before annealing in Fig. 1 were regarded as the experimental transition temperature in Fig. 3(a) because the temperatures in Fig. 1 seem to be less affected by the time lag in scanning methods than those temperatures in Fig. 2 for samples after annealing. These experimental transition temperatures are in good agreement with those observed previously by Hirabayashi et al. [6]. However, the experimental transition enthalpy and entropy changes obtained in this study are larger than those reported by Hirabayashi et al. [6]. This fact may be caused by the

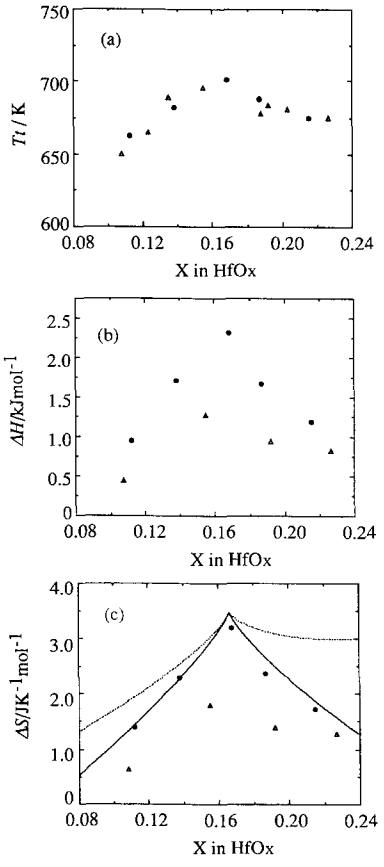

Fig. 3. (a) Transition temperatures (T_t), (b) transition enthalpy changes (ΔH) and (c) transition entropy changes (ΔS) of HfO_X as a function of O/Hf atomic ratios. (●) T_t, ΔH and ΔS in this work. (△) T_t, ΔH and ΔS by Hirabayashi et al. [6]. ————: Theoretical transition entropy change calculated on the basis of crystal analyses. · · ·: Transition entropy change calculated using the equations proposed in this work.

difference in the starting materials, annealing condition and the estimation of base line.

We can calculate the theoretical transition entropy changes by using statistical thermodynamics from configurational entropy changes for the interstitial oxygen atoms in host hafnium lattice between the ordered and disordered phase, on the basis of crystal analyses. The equations used for the calculation are as follows [6]:

$$X \le 1/6, \quad \Delta S = k\{\ln({}_{N-NX}C_{NX})\} - k\{\ln({}_{N/6}C_{NX})\},$$

$$X > 1/6, \quad \Delta S = k\{\ln({}_{N-NX}C_{NX})\} - k\{\ln(N_X C_{n(X-1/6)})\},$$

where k and N are Boltzmann's constant and Avogadro's number, respectively. On the right hand side in these equations, the first and second terms are derived from the configurational entropies of the disordered and ordered phase, respectively. The theoretical value is shown as the dotted line in Fig. 3(c). The experimental transition entropy change for the composition of $X = 0.17$ ($\approx 1/6$) is in good agreement with the theoretical value. It seems that the heat capacity data measured in this study are carried out on the samples annealed sufficiently at more appropriate temperature to form the order structures. This fact implies that the order–disorder transition takes place following the transition mechanism on the basis of the crystal analyses for $HfO_{1/6}$ and $HfO_{1/6}$ has a complete ordered structure whose configurational entropy is zero as reported by Hirabayashi et al. [6]. It has not been confirmed that titanium- and zirconium–oxygen solid solutions have complete ordered structures for the composition of O/M = 1/6 and the existence of the complete ordered structure for $HfO_{1/6}$ may imply that the repulsive force between interstitial oxygen atoms in HfO_X is stronger than those in TiO_X or ZrO_X.

On the other hand, the experimental transition entropy changes for other compositions ($X \neq 0.17$) are smaller than the theoretical values, respectively. For the composition of $X = 0.14$, the experimental transition entropy change in our previous estimation was in good agreement with the theoretical value, however after the computation using the attenuation line the experimental transition entropy change is smaller than the theoretical value, because the low temperature heat capacity anomaly had less influence on the computation of the experimental transition entropy change in consideration of the attenuation line in this study than that in our previous work. We propose the increasing degree of configurational freedom of the ordered structures as one of the explanations for the difference between the experimental and theoretical transition entropy changes. Assuming that factor 'α' is the number of the increasing degree per one oxygen vacancy (or one interstitial oxygen atom) for $X \le 1/6$ (or $X > 1/6$), compared to the basic ordered structure for $X = 1/6$, the equations for the transition entropy change are expressed as

$$X \le 1/6, \quad \Delta S = k\{\ln({}_{N-NX}C_{NX})\} - k\{\ln({}_{N/6}C_{NX})\,\alpha^{N(1/6-X)}\},$$

$$X > 1/6, \quad \Delta S = k\{\ln({}_{N-NX}C_{NX})\} - k\{\ln({}_{NX}C_{N(X-1/6)})\,\alpha^{N(X-1/6)}\}.$$

The transition entropy changes calculated using these equations in the case of $\alpha = 3$ for $X \le 1/6$ and $\alpha = 17$ for $X > 1/6$ are shown as the solid line in Fig. 3(c). These calculated transition entropy changes fit to the experimental values very well.

We can not discuss, in more detail, the order–disorder transition mechanism. However, it can be remarked that the interstitial oxygen atoms or the oxygen vacancies, compared to the basic ordered structure for $X = 1/6$,

break the balance of the strong repulsive force between the interstitial oxygen atoms in hafnium metal, affect the configuration of the oxygen originally occupied the interstitial sites in the basic ordered structure for $X = 1/6$ and then cause the increasing degree of configurational freedom of the ordered structures.

4. Conclusions

We measured heat capacities of hafnium–oxygen solid solutions, HfO_X ($X = 0.11$, 0.19 and 0.22) from 325 to 905 K and computed the entropy changes due to the order–disorder transition of oxygen sublattice from heat capacity data, including HfO_X ($X = 0.14$ and 0.17) measured in our previous study.

(1) The experimental transition entropy change for $X = 0.17$ ($\approx 1/6$) was in good agreement with the theoretical value calculated on the basis of the crystal analyses using statistical thermodynamics. The fact may imply that $HfO_{1/6}$ has a complete ordered structure whose configurational entropy is zero.

(2) The experimental transition entropy for $X = 0.11$, 0.14, 0.19 and 0.22 were smaller than the theoretical value. The difference between the experimental and theoretical transition entropy changes may be caused by the increasing degree of configurational freedom of the ordered structure.

Acknowledgements

The authors are indebted to Dr K. Abe of Kobe Steel Ltd, Hyogo, Japan for sample preparation.

References

[1] T. Tsuji, M. Sato, K. Naito, Thermochim. Acta 163 (1990) 279.
[2] T. Tsuji, M. Amaya, K. Naito, J. Thermal Anal. 38 (1992) 1817.
[3] R.F. Domagala, R. Ruh, ASM Trans. Q. 58 (1965) 164.
[4] E. Rudy, P. Stecher, J. Less Common Met. 5 (1963) 78.
[5] G. Boureau, P. Gerdanian, J. Phys. Chem. Solids 45 (1984) 141.
[6] M. Hirabayashi, S. Yamaguchi, T. Arai, J. Phys. Soc. Jpn. 35 (1973) 473.
[7] T. Kato, T. Tsuji, Thermochim. Acta 267 (1995) 397.
[8] T.B. Douglas, J. Natl. Bur. Standards A67 (1963) 403.